Research article

SURFACE and INTERFACE ANALYSIS

Received: 13 February 2012 Revised: 16 August 2012 Accepted: 16 August 2012 Published online in Wiley Online Library: 4 September 2012

(wileyonlinelibrary.com) DOI 10.1002/sia.5164

Systematic calculation of the surface excitation parameters for 22 materials

B. Da, Y. Sun, S. F. Mao and Z. J. Ding*

Quantitative surface analysis requires knowledge of surface excitations by electrons. These excitations are characterized by the surface excitation parameter (SEP) which represents the surface excitation probability while an electron moves across a solid surface. In this work, a systematic calculation of a SEP database has been performed for 22 materials, including metals, oxides and semiconductors, for electron energies between 100 eV and 5000 eV, and for angles α of incidence/emission between 0.5° and 89.5° with respect to the surface normal. Surface excitations are considered for both sides of a solid–vacuum interface when an electron is incident on or emitted from a surface. These SEPs represent not only the appearance of surface excitations but also the inhibition of bulk excitations. Four common SEP formulas are evaluated, and we present best-fit parameters for the most satisfactory formula. SEP can then be readily determined for about 22 materials and various energies and electron incidence or emission angles. Copyright © 2012 John Wiley & Sons, Ltd.

Keywords: surface excitation; surface excitation parameter; SEP database; dielectric function

Introduction

Knowledge of inelastic electron scattering plays an important role in surface-sensitive spectroscopies, such as X-ray photoelectron spectroscopy, Auger electron spectroscopy, elastic-peak electron spectroscopy (EPES) and reflection electron energy-loss spectroscopy (REELS). Electron signals in all these electron spectroscopies are influenced predominantly by the electron inelastic mean free path (IMFP). Consequently, many theoretical and experimental works have been done in order to acquire more precise IMFP values. However, there is still a discrepancy of IMFP data between theoretical calculation and experimental measurement, which has been attributed to different sources, e.g. accuracy of electron elastic-scattering cross sections,[1] the dielectric function model[2] and surface roughness.[3,4] According to previous studies,[5–8] surface excitations which occur due to electrons crossing the interface of two different materials are likely to be the major reason for the deviations. Therefore, it is necessary to quantitatively estimate the surface excitation effect.

To characterize the surface excitation probability, the surface excitation parameter (SEP) was introduced, which was defined as the average number of excitations generated by an electron moving across the solid surface once.[9–11] Tung[9] considered the surface excitation effect in an oversimplified model in which the surface excitations occur just at the surface boundary without extending to both sides of the surface boundary. Chen and Kwei[10,12,13] used a semi-classical expression of the position-dependent differential inverse IMFP (DIIMFP) to evaluate the surface excitation effect, which decays exponentially on both the vacuum and solid sides. The SEPs were calculated by an integration of the inverse IMFP over the electron path length in vacuum only. All the SEP results mentioned above have been calculated by assuming that the appearance of surface excitations inside the solid compensates exactly the decrease in volume excitations. However, according to this approximation, the extent of the surface excitation effect which suppresses volume excitations, i.e. the Begrenzungs (boundary) effect,[14,15] has been underestimated especially for nonmetallic materials. An alternative definition of the SEP, which accounts for the Begrenzungs effect, has been given by Pauly and Tougaard.[16] By considering the overall change in the excitation inside the solid, i.e. appearance of surface excitation with reduction of volume excitation, this definition is more reasonable and precise for the description of surface excitations, especially for nonmetallic materials.

In our previous works,[17–19] the position-dependent DIIMFP was obtained based on quantum self-energy formalism. Then, a comparison[20] of the DIIMFP and IMFP in the vicinity of the surface was made between the quantum-mechanical approach and a semi-classical approach.[21] Furthermore, Monte Carlo simulations of REELS spectra were performed based on these two approaches, and the results were compared with experimental spectra; the simulations indicated that the calculation results by these two methods are effectively quite close to each other in most cases. Although the calculation based on the quantum-mechanical approach is more accurate, it is impractical to be adopted for SEP database calculations because of its low computation efficiency.

In the present study, therefore, the semi-classical method is applied to derive a SEP database which allows a simple numerical calculation. The crossing-angle- and energy-dependent SEPs for 22 materials, including metals, oxides and semiconductors for electron energies between 100 eV and 5000 eV, and for angles between 0.5° and 89.5° to the surface normal, are calculated. Some of the SEPs are compared with published data even though the SEP

* Correspondence to: Z. J. Ding, Hefei National Laboratory for Physical Sciences at Microscale and Department of Physics, University of Science and Technology of China, 96 Jinzhai Road, Hefei, Anhui 230026, P.R. China.
E-mail: zjding@ustc.edu.cn

Hefei National Laboratory for Physical Sciences at Microscale and Department of Physics, University of Science and Technology of China, 96 Jinzhai Road, Hefei, Anhui, 230026, P.R. China

definitions may differ. We also assess four common formulas for fitting the calculated SEPs; parameters for the best-fitted formula for various materials are then given.

Theoretical method

Many theoretical works[5,6,14,22–26] have been performed in order to understand the interaction of external electrons with a semi-infinite medium in the framework of classical electrodynamics. Here, we consider an electron moving across a solid surface with an energy E at an angle α with respect to the surface normal. The solid medium is considered to occupy a semi-infinite space with the surface boundary defined at $z=0$. The solid is characterized by its dielectric function, $\varepsilon(\mathbf{q},\omega)$, where $\mathbf{q}$ is the momentum transfer and ω is the energy transfer. Figure 1 shows a sketch of the considered geometry with the vacuum ($z>0$) and solid ($z<0$) regions in case of electron incidence ($v_\perp<0$).

In this work, the SEP is calculated by an integration of the surface excitation part of the DIIMFP both inside and outside the solid, including the Begrenzungs effect inside the solid. The SEPs, P_s, for escaping electrons (from solid to vacuum: $S\rightarrow V$) and incoming electrons (from vacuum to solid: $V\rightarrow S$) can be expressed by, respectively,[27]

$$P_s^{S\rightarrow V}=\frac{8\cos\alpha}{\pi^2}\int_0^E d\omega\int_{q_-}^{q_+}dq\int_0^{\pi/2}d\theta\times\left\{\left[\mathrm{Im}\left\{\frac{-1}{\varepsilon(\mathbf{Q},\omega)+1}\right\}\left(\sin^2\theta-\frac{1}{2}\right)-\frac{1}{2}\mathrm{Im}\left\{\frac{-1}{\varepsilon(\mathbf{Q},\omega)}\right\}\right]\frac{\sin\theta\sin\varphi\sin\alpha}{BQ^2v_\perp{}^2\cos^2\alpha}\right.$$
$$\left.+\mathrm{Im}\left\{\frac{-1}{\varepsilon(\mathbf{Q},\omega)+1}\right\}\frac{\tan\alpha}{q^2v^2\sin\theta}\left[\frac{\sin\varphi\tan\alpha}{B}-\frac{1}{B^3}\left(\frac{\omega}{Qv_\parallel}\cos3\varphi+\cot\alpha\sin3\varphi\right)\right]\right\} \quad (1)$$

and

$$P_s^{V\rightarrow S}=\frac{8\cos\alpha}{\pi^2}\int_0^E d\omega\int_{q_-}^{q_+}dq\int_0^{\pi/2}d\theta\times\left\{\left[\mathrm{Im}\left\{\frac{-1}{\varepsilon(\mathbf{Q},\omega)+1}\right\}\left(\sin^2\theta-\frac{1}{2}\right)+\frac{1}{2}\mathrm{Im}\left\{\frac{-1}{\varepsilon(\mathbf{Q},\omega)}\right\}\right]\frac{\sin\theta\sin\varphi\sin\alpha}{BQ^2v_\perp{}^2\cos^2\alpha}\right.$$
$$\left.+\left[\mathrm{Im}\left\{\frac{-1}{\varepsilon(\mathbf{Q},\omega)+1}\right\}-\frac{1}{2}\mathrm{Im}\left\{\frac{-1}{\varepsilon(\mathbf{Q},\omega)}\right\}\right]\frac{\tan\alpha}{q^2v^2\sin\theta}\left[\frac{\sin\varphi\tan\alpha}{B}-\frac{1}{B^3}\left(\frac{\omega}{Qv_\parallel}\cos3\varphi+\cot\alpha\sin3\varphi\right)\right]\right\} \quad (2)$$

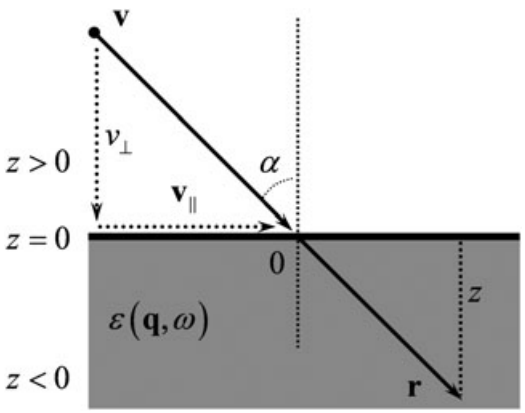

Figure 1. A sketch of the geometry of movement of an electron with a velocity $\mathbf{v}=(\mathbf{v}_\parallel,v_\perp)$ at a position $\mathbf{r}=\mathbf{v}t$ measured from the origin on a surface ($z=0$).

where

$$B=\sqrt[4]{\left(\frac{\omega^2}{Q^2v_\parallel{}^2}+\cot^2\alpha\right)^2-2\left(\frac{\omega^2}{Q^2v_\parallel{}^2}+\cot^2\alpha\right)+4\cot\alpha+1} \quad (3)$$

$$\varphi=\sin^{-1}\left(\sqrt{\frac{B^2Q^2v_\parallel{}^2\sin^2\alpha-\omega^2\sin^2\alpha+Q^2v_\parallel{}^2}{2B^2}}\right) \quad (4)$$

and $Q=q\sin\theta$, $v_\parallel=v\sin\alpha$ and $v_\perp=v\cos\alpha$. v is electron velocity and $E=v^2/2$ is electron kinetic energy. According the energy-momentum conservation relations, the upper and lower limits of q are given by $q_\pm=\sqrt{2E}\pm\sqrt{2(E-\omega)}$. Atomic units are used throughout this paper unless otherwise specified. From the above formulae, it can be seen that the dielectric function $\varepsilon(\mathbf{q},\omega)$ is obviously the only material factor in determining SEP. $\varepsilon(\mathbf{q},\omega)$ can be obtained by extrapolating experimental values of the optical dielectric function $\varepsilon(\omega)$ from the optical limits to other momentum transfers. To do this, Ritchie and Howie's approach[28] is employed for obtaining an approximate energy loss function, $\mathrm{Im}\{-1/\varepsilon(\mathbf{q},\omega)\}$, from an optical energy loss function, $\mathrm{Im}\{-1/\varepsilon(\omega)\}$. A bulk energy loss function is first decomposed into N terms of the Drude-Lindhard model energy loss function:

$$\mathrm{Im}\left\{\frac{-1}{\varepsilon(q,\omega)}\right\}=\sum_{i=1}^{N}a_i\mathrm{Im}\left\{\frac{-1}{\varepsilon(q,\omega;\omega_{pi},\gamma_i)}\right\} \quad (5)$$

where the $3N$ parameters, a_i, γ_i and ω_{pi} are, respectively, the oscillator strength, width and energy of the *ith* oscillator. These parameters are determined from an experimental optical energy loss function taken from a database[29] by using the fitting procedure below:

$$\mathrm{Im}\left\{\frac{-1}{\varepsilon(\omega)}\right\}=\sum_{i=1}^{N}a_i\mathrm{Im}\left\{\frac{-1}{\varepsilon(0,\omega;\omega_{pi},\gamma_i)}\right\} \quad (6)$$

An example of such fitting for SiO_2 over a wide energy loss range covering phonon and plasmon excitations, interband transition and inner shell ionization is given in Fig. 2. Energy loss functions for the same optical data[29] fitted by different dielectric models in Kwei's[30] and Pauly's[31] works are also presented here for

SURFACE and INTERFACE ANALYSIS

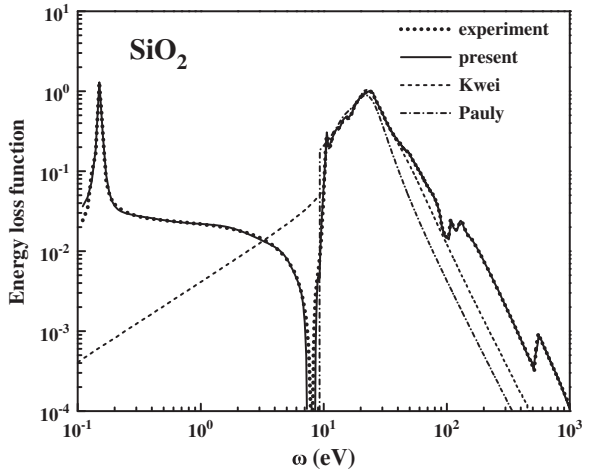

Figure 2. A comparison on the optical energy loss function Im[$-1/\varepsilon(\omega)$] among experimental data,[29] present fitting results, Kwei's results[30] and Pauly's results[31] for silicon dioxide.

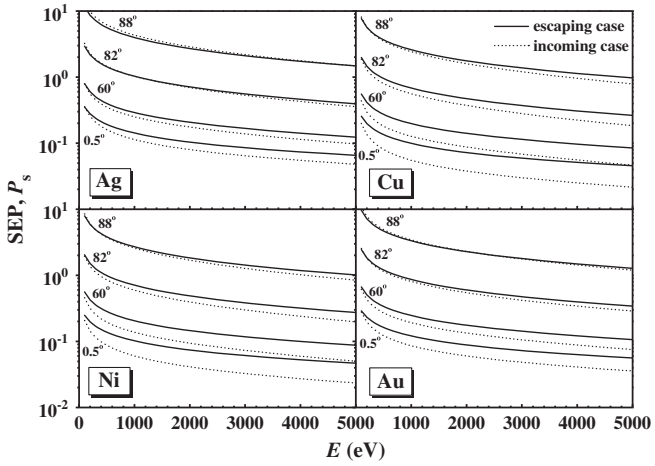

Figure 3. Comparisons of the SEP energy dependence for the escaping and incoming cases for Ag, Cu, Ni and Cu at different crossing angles with respect to the surface normal direction.

comparison. The oscillator strength (*f*-sum) and perfect-screening sum (*ps*-sum) rules for both optical measurements and our fitted data of 22 materials are given in Table 1.

Results and discussion

Based on the dielectric response theory, the energy-dependent SEP is calculated using the optical dielectric function. In Fig. 3, SEPs for metallic materials, Ag, Cu, Ni and Au, are shown for both the electron incidence and emission cases. It is found that the surface excitation is stronger in the emission case than in the incidence case, especially for fast electrons moving close to the normal direction to the surface. The asymmetry of this angular dependence of SEP on electron-moving direction originates from the induced surface charges, which provides an attractive force on electrons moving in vacuum towards the surface. The action effectively speeds up the incident electrons but slows down the escaping electrons. Thus, the time spent in the surface region is longer, and the surface excitation is greater for escaping electrons than for incident electrons. As shown by Fig. 4, the difference of the SEPs between the incidence case and emission cases is even larger for

Table 1. Evaluations of the *f*-sum and *ps*-sum rules from both optically measured ELFs and our fitted ELFs for 22 materials together with the corresponding errors

N	Element	*f*-sum				*ps*-sum			
		Optical	Error	Fitted	Error	Optical	Error	Fitted	Error
12	Mg	15.713	30.9%	15.546	29.6%	1.013	1.3%	1.011	1.1%
13	Al	12.748	−1.9%	12.742	−2.0%	1.000	0.0%	1.000	0.0%
14	Si	13.713	−2.1%	13.749	−1.8%	0.878	−12.2%	0.882	−11.8%
26	Fe	23.443	−28.7%	23.387	−10.1%	0.868	−13.2%	0.868	−13.2%
27	Co	19.252	−28.7%	21.46	−20.5%	0.832	−16.8%	0.833	−16.7%
28	Ni	26.509	−5.3%	26.475	−5.4%	1.022	2.2%	1.022	2.2%
29	Cu	35.64	22.9%	34.114	17.6%	1.001	0.1%	1.001	0.1%
30	SiO_2	28.456	−5.1%	28.476	−5.1%	0.691	−30.9%	0.703	−29.7%
41	Nb	36.856	−10.1%	36.293	−11.5%	0.834	−16.6%	0.826	−17.4%
42	Mo	35.778	−14.8%	35.271	−16.0%	0.963	−3.7%	0.963	−3.7%
46	Pd	31.576	−31.4%	31.255	−32.1%	1.127	12.7%	1.126	12.6%
46	ZnS	44.570	−3.1%	44.906	−2.4%	0.686	−31.4%	0.697	−30.3%
47	Ag	51.476	9.5%	50.886	8.3%	1.153	15.3%	1.153	15.3%
50	Al_2O_3	45.054	−9.9%	45.01	−10.0%	2.085	108.5%	2.102	110.2%
52	Te	61.811	18.9%	57.647	10.9%	1.464	46.4%	1.464	46.4%
55	Cs	47.427	−13.8%	45.509	−17.3%	1.000	0.0%	0.997	−0.3%
64	AgCl	56.740	−11.3%	59.541	−7.0%	0.904	−9.6%	0.889	−11.1%
64	ZnSe	44.193	−30.9%	44.381	−30.7%	0.701	−29.9%	0.703	−29.7%
68	Er	64.824	−4.7%	63.169	−7.1%	1.074	7.4%	1.075	7.5%
78	Pt	73.887	−5.3%	73.442	−5.8%	1.112	11.2%	1.113	11.3%
79	Au	71.701	−9.2%	71.947	−8.9%	1.091	9.1%	1.091	9.1%
82	ZnTe	63.291	−22.8%	62.464	−23.8%	0.840	−16.0%	0.842	−15.8%

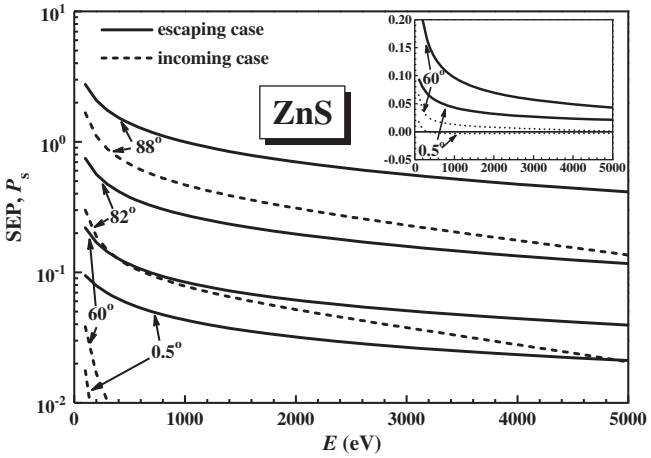

Figure 4. Comparison of the energy dependence of the SEP for electrons escaping from ZnS into vacuum and incoming onto ZnS from vacuum at different crossing angles with respect to the surface normal direction.

semiconductors, such as ZnS, especially at small crossing angles. It can also be found that the SEP for the incidence case decreases more rapidly with the energy of electrons, especially at a small incident angle. In this case, the reduction of the bulk excitation inside the sample is comparable with the surface excitation, and even stronger at a small incident angle. Hence, the net total excitation probability is negligible and even negative in the incidence case at a small incident angle. It is obvious that the Begrenzungs effect is more important for a semiconductor than for a metal. Hence, it is reasonable to calculate the SEP, including the change in the excitation probability inside the sample, instead of considering the surface excitation only in vacuum, especially for nonmetallic materials.

Here, comparisons are made in Figs. 5 and 6 between the present SEPs and earlier work published by Kwei[32] and Werner.[33] It is noteworthy that in Kwei's work, the SEPs are calculated only considering surface excitation that occurs in vacuum. Here, our SEPs are

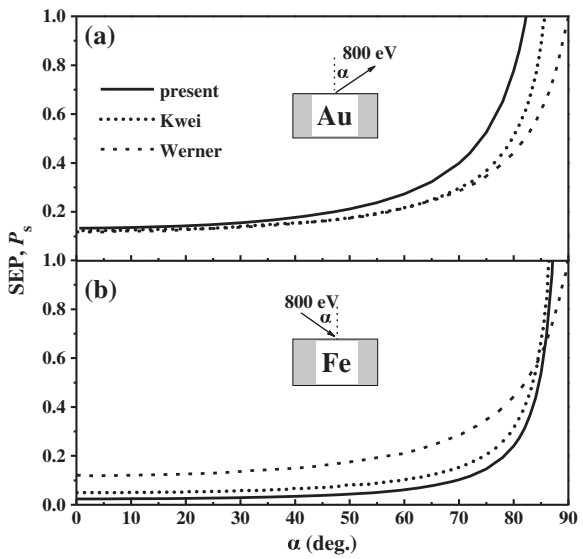

Figure 5. Comparisons of the angular dependence of SEP between the present work, Kwei[29] and Werner[32] for electrons of 800 eV (a) escaping into vacuum from the Au surface and (b) incident on the Fe surface from vacuum.

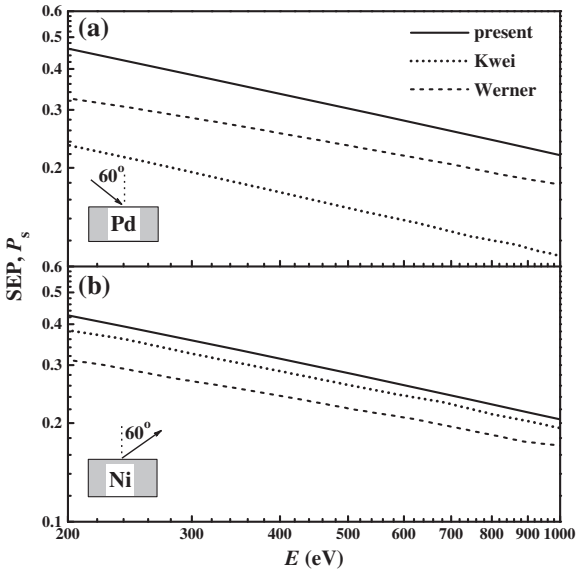

Figure 6. Comparisons of the energy dependence of SEP between the present work, Kwei[29] and Werner[32] for electrons (a) incident on the Pd surface from vacuum and (b) escaping into vacuum from the Ni surface.

calculated by also considering the change in the excitation probability inside the solid, which is important in the incidence case. In Fig. 5, there is no significant difference among the three SEPs for Au in the emission case at a small emission angle, but the deviations increase with increasing emission angle. However, for electrons incident on a Fe surface, the differences are large for all incidence angles due to the Begrenzungs effect which is more important in incidence case. As shown in Fig. 6, the differences in SEP between Kwei's results and ours are larger for the incidence case than the emission case, due to the asymmetry of the electron moving direction.

Figure 7 shows the total surface excitation probability for electron trajectories reflected from the surface, where surface losses are considered for electrons in both incident and escaping direction; comparisons are also made with reported experimental SEP values in the literature. The SEPs of Salma *et al.* were calculated by quantum-mechanical methods,[11] while the semi-classical method is used in the present work instead. It is seen that, under the same definition of the SEP, there is a small difference between the present results and those from Salma *et al.* Figures 8(a) and 8(b) provide comparison of the present calculations with the calculated values of Chen[34] and the experimental results of Gergely *et al.* [35] for Ag and Cu, respectively. The total SEP as a function of the electron energy for $\alpha_i = 50^o$ and $\alpha_o = 0^o$ is plotted using the formula of Gergely *et al.* and parameters provided in their work. The present calculations of the total SEP for Cu are in reasonable agreement with Chen[34] and also reasonably close to Gergely's results for Cu at low electron energies. However, in the case of Ag, our results are much larger than their results. Figures 7(c) and 8(d) present a comparison of our SEP values with the experimental results of Werner *et al.*,[33,36] which were obtained by fitting REELS experimental data according to the theory of Tung *et al.*,[9] for Au and Cu, respectively. Our calculated results of the SEP for $\alpha_i = 0^o$ and $\alpha_o = 60^o$ are in good agreement with their raw experimental data for Au and Cu. In the present calculation of the surface excitation probability, surface excitation events occurring in the bulk and vacuum region are considered, whereas, only the vacuum region was considered in Kwei's, Chen's and Gergely's work.[35] More

SURFACE and INTERFACE ANALYSIS

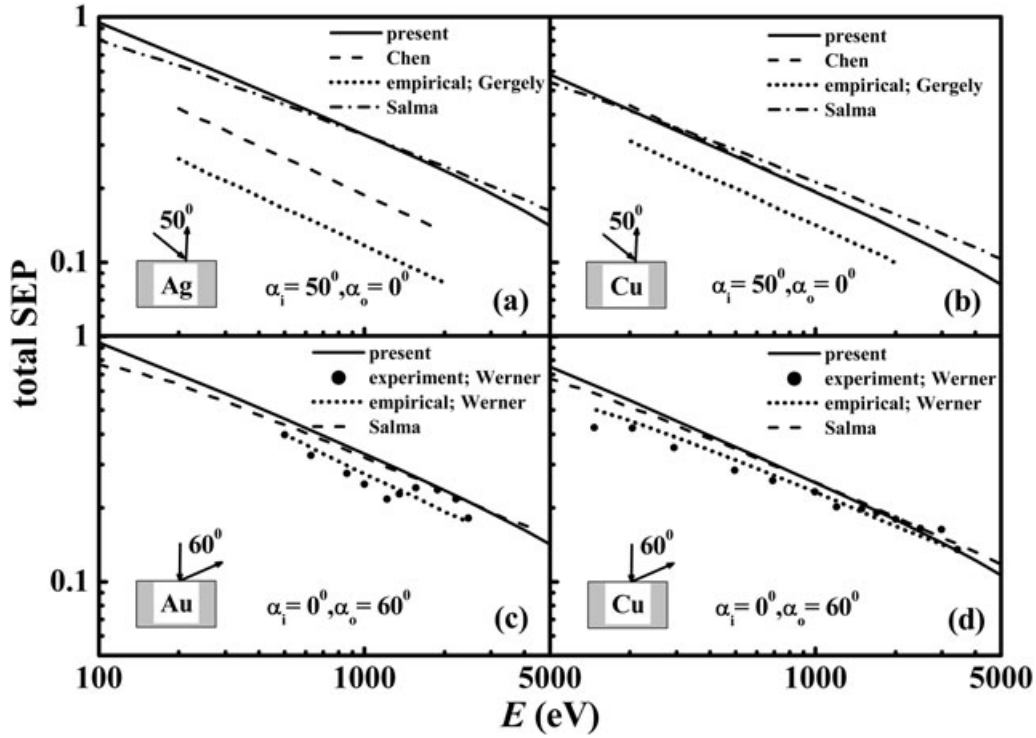

Figure 7. Comparisons of total SEPs as a function of electron energy with other results from Refs. [11,32–35] for different incidence and emission angles of electrons. (a) Ag; (b) Cu; (c) Au; (d) Cu.

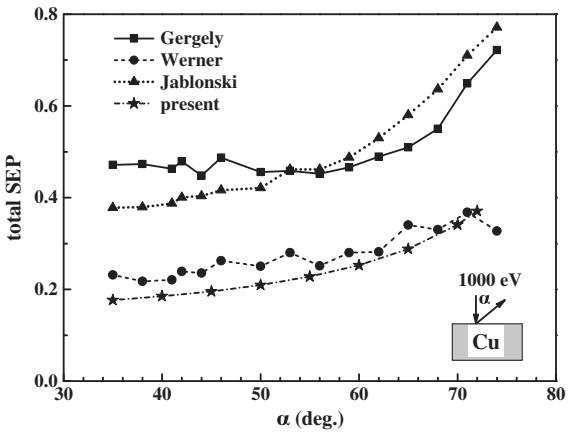

Figure 8. Comparisons of the angular dependence of the SEP for 1-keV electrons escaping from Cu surfaces from Werner *et al.*,[37] Jablonski and Zemek,[38] Gergely *et al.*[39] and the present work.

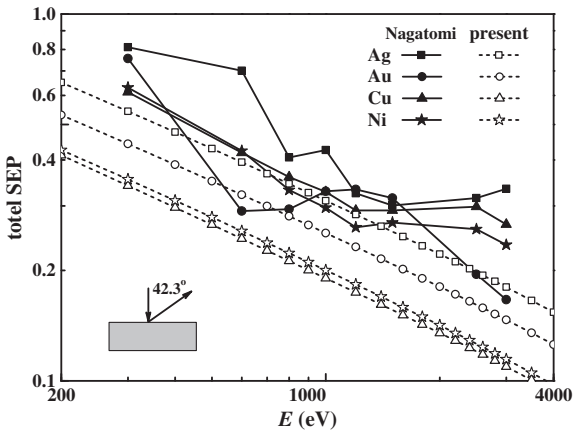

Figure 9. Comparisons of the energy dependence of SEPs from the present calculation and the experimental results of Nagatomi *et al.*[40] measured by a CMA with a Faraday cup.

recent experimental results[37–39,42] of total SEP for Cu are presented in Fig. 8. Our calculated result is close to Werner's new data.[37] While Jablonski's data[38] and Gergely's results[39] are larger, the deviations between the last two results are not significant since they are based on the same set of measured angular-resolved spectra. Comparisons of total SEPs for Ag, Au, Cu and Ni with the experimental results of Nagatomi *et al.*[40] are given in Fig. 9. The SEPs in Nagatomi's work were determined from absolute measurements of REELS spectra that were analyzed with Landau theory. Our calculated results are smaller than the experimental values of Nagatomi in most cases. The measured SEPs values of Nagatomi *et al.* generally decrease with increasing electron energy, due to the influence of elastic scattering.

Pauly and Tougaard[31,41,42] have also performed SEP calculations by using the definition of the SEP as the change in the excitation probability. This definition contains the change in excitation inside the solid. However, their calculations are made under the assumption of equal contribution to the SEP by incoming and outgoing electrons. This assumption does not hold for fast electrons and at a small crossing angle with respect to the surface normal direction, especially for electrons incident on semiconductor materials. Figure 10 shows a comparison between the present SEP values and Pauly and Tougaard's data for several metals. Because the difference in the SEP for metals between incoming and outgoing electrons is small, we compare the outgoing SEP with their results. The SEP increases with crossing angle, because the time spent in

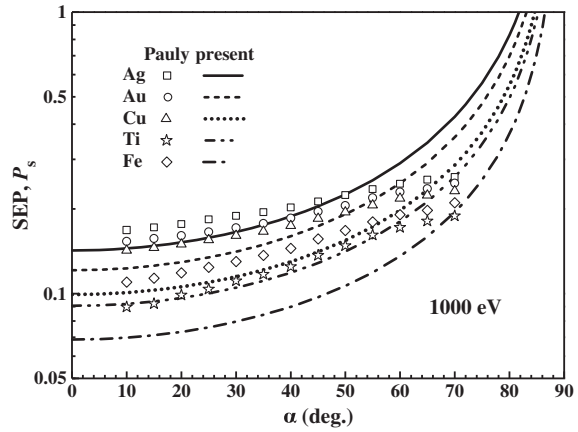

Figure 10. Comparisons of the angular dependence of the SEP for 1000-eV electrons escaping from Ag, Au, Cu, Ti and Fe surfaces from the present work, and from Pauly and Tougaard.[36]

the surface region is increased also. The tendency for increasing SEP is more rapid at large crossing angles than found by Pauly and Tougaard. As shown in Fig. 3, the SEP in the emission case is a little larger than the incident case for most metals; however, there is no such consistency for semiconductors, due to the more important role of the Begrenzungs effect. Figure 11 shows the SEP for three semiconductor materials. It is found that the SEP in the incoming case is larger than the emission case for Si, but the situation is more complicated for ZnS and ZnSe: the SEP for incident electrons is smaller for small crossing angles but larger for higher crossing angles. It is should be noted that different energy loss functions were employed by different authors, and this could explain some of the deviations presented above.

For practical applications, it is useful to have a simple formula that fits the SEPs calculated here. There are now four other formula for the SEP:

(1) Chen's formula:[34]

$$P_s(E,\alpha) = \frac{a}{\sqrt{E}\cos\alpha} \tag{7}$$

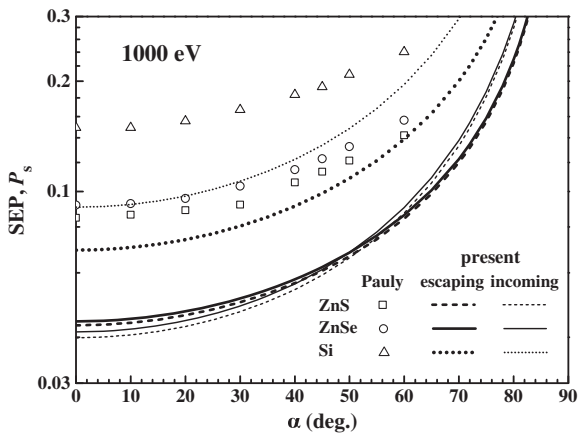

Figure 11. Comparisons of the angular dependence of the SEP for 1000 eV incoming to and escaping from ZnS, ZnSe and Si surfaces from the present work, and Pauly and Tougaard.[41]

(2) Kwei's formula:[32]

$$P_s(E,\alpha) = \frac{aE^{-b}}{\cos^c\alpha} \tag{8}$$

(3) Salma *et al.* formula:[11]

$$P_s(E,\alpha) = a(\alpha)\sec\alpha E^{-b(\alpha)};\quad a(\alpha) = a_1 - a_2\cos\alpha;\quad b(\alpha) = b_1 - b_2\cos\alpha \tag{9}$$

(4) Werner's formula:[33]

$$P_s(E,\alpha) = \frac{1}{0.173a\sqrt{E}\cos\theta + 1} \tag{10}$$

where P_s is the SEP, E is the electron energy (in eV), α is the angle between the electron trajectory and the surface normal, $a(\alpha)$ and $b(\alpha)$ are material- and angle-dependent parameters, and a, b, c, a_1, a_2, b_1 and b_2 are all material-dependent parameters for the incident and emission cases. In order to find out which formula fits the calculated data best, we have evaluated the fitting by calculating the root-mean-square, *RMS*, and mean percentage deviations, *R*:

$$RMS = \sqrt{\frac{1}{n}\sum_{i=1}^{n}(SEP_c - SEP_i)^2} \tag{11}$$

$$R = 100\frac{1}{n}\sum_{i=1}^{n}\left|\frac{SEP_c - SEP_i}{SEP_c}\right| \tag{12}$$

where SEP_c represents the value calculated directly from Eqns (1) and (2), and SEP_i is the interpolated result from a fitting formula.

Evaluated *RMS*- and *R*-values are shown in Figs. 12 and 13, respectively, for metallic and nonmetallic materials. Considering most experimental configurations, SEPs with a crossing angle less than 70° are more important. Therefore, the assessment of the effectiveness of fit formulas is also made for crossing angles less than 70°. In Fig. 12, it is evident that for metals, the incoming SEPs are fitted better for small crossing angles, but the outgoing SEPs seem better fitted for large crossing angles. Kwei's and Salma's formulas are better than Chen's and Werner's in describing the calculated SEPs. In Fig. 13, because of the complicated Begrenzungs effect for nonmetals, for example, SEPs are poorly fitted by these four formulas. For nonmetals, results from the four formulas do not present large differences as for metals. Therefore, in the present work, we have chosen the formula of Salma *et al.* to fit the SEPs calculated for all 22 materials considered here, the electron energy range 100–5000 eV and full range of crossing angles. The total SEP can be found by using Eqn (9) and the parameters in Table 2 to sum the SEPs for the incidence and emission cases.

Conclusions

In this work, systematic calculations of SEPs for 22 materials and the electron energy range 100–5000 eV have been performed based on a semi-classical algorithm that uses an integration of the surface excitation part of the DIIMFP both inside and outside the solid. This SEP can describe the change in the excitation probability including the Begrenzungs effect. The influence of the Begrenzungs effect is discussed according to this definition of the SEP, and it is found that the Begrenzungs effect is more

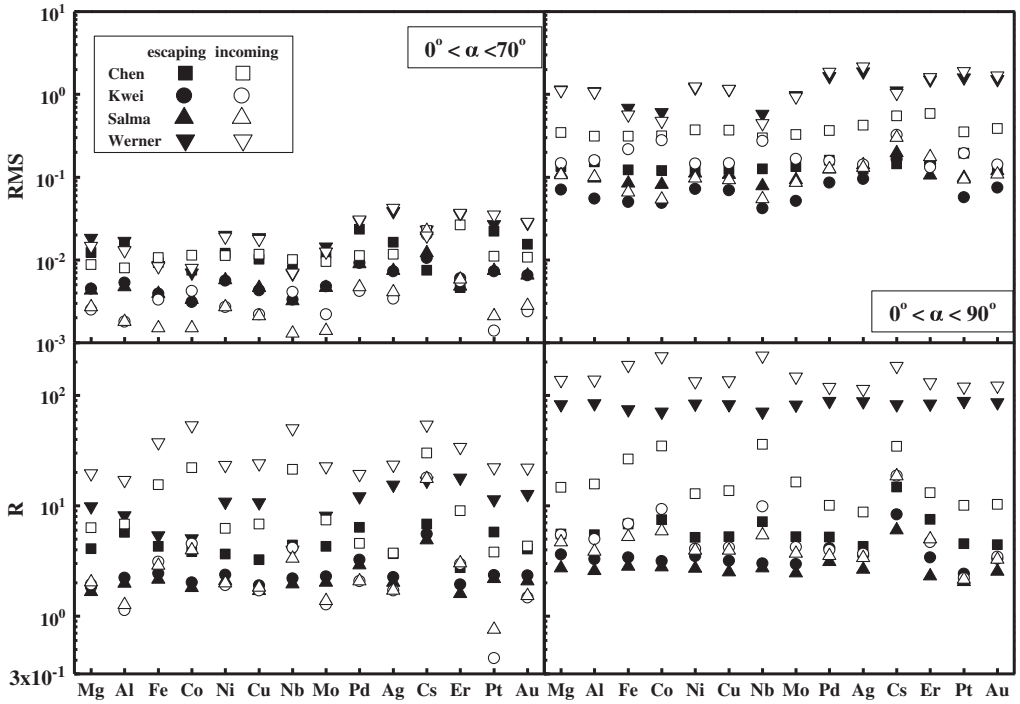

Figure 12. Values of root-mean-square, *RMS*, and mean percentage deviations, *R*, for four formulas best fitted to our calculated SEP data for 14 metallic materials in both the escaping and incoming cases for 100–5000 eV electrons. The left panels are for crossing angles α less than 70° and the right panels for the full range of crossing angle.

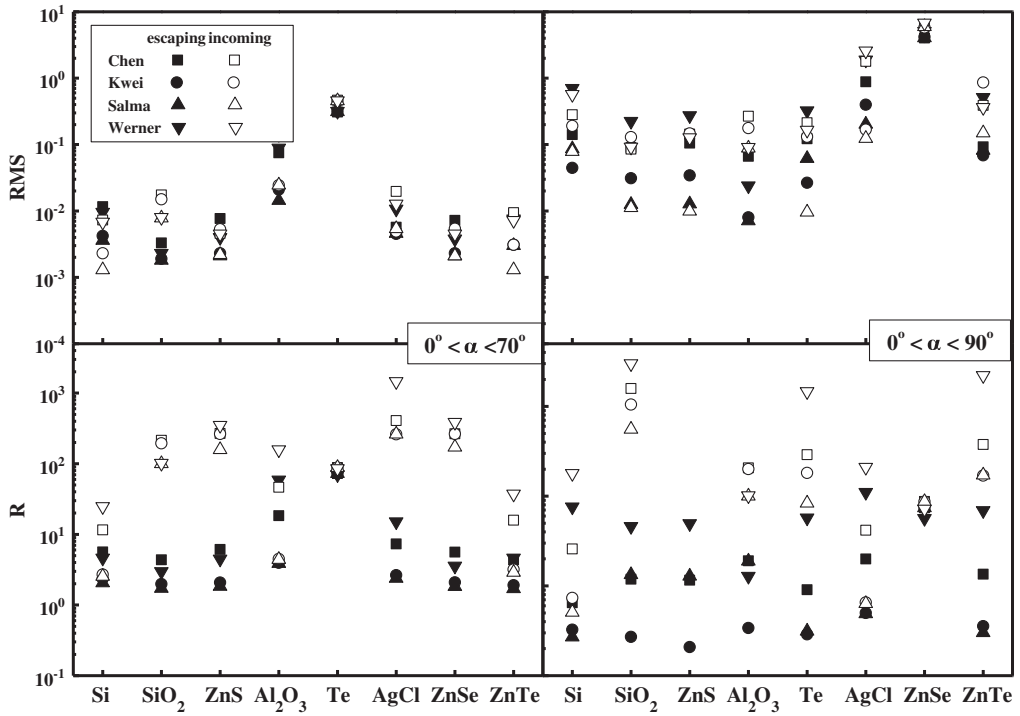

Figure 13. Values of root-mean-square, *RMS*, and mean percentage deviations, *R*, for four formulas best fitted to our calculated SEP data for eight nonmetallic materials in both the escaping and incoming cases for 100–5000 eV electrons. The left panels are for the crossing angles α less than 70° and the right panels for the full range of crossing angle.

important for fast electrons incident on or escaping from a surface at a small crossing angle with respect to surface normal, especially for nonmetals. Hence, SEPs for nonmetals differ larger with varying electron moving direction due to the more important role played by the Begrenzungs effect. Furthermore, available theoretical and experimental data for the SEP based on different definitions are compared with our present calculations, and good agreement is found between our results and

Table 2. Best-fit parameters in Eqn (9) for both incidence and emission cases

	Emission case				Incidence case			
	a1	a2	b1	b2	a1	a2	b1	b2
Ag	5.03	2.92	0.54	0.14	7.35	2.23	0.58	−0.01
AgCl	2.75	1.35	0.63	0.17	3.42	0.81	0.69	−0.50
Al2O3	13.6	7.49	0.78	0.12	57.1	13.5	1.01	−0.14
Al	2.59	1.68	0.50	0.17	3.12	0.78	0.54	−0.08
AlAs	0.18	0.14	0.45	0.31	0.10	0.34	0.57	−0.99
Au	3.94	2.35	0.53	0.15	5.72	1.55	0.57	−0.03
CdS	1.34	0.80	0.52	0.18	1.59	0.73	0.54	0.03
Cu	3.31	1.95	0.54	0.16	4.88	1.13	0.60	−0.07
Cs	7.34	3.85	0.66	0.13	10.2	5.26	0.66	0.12
Co	1.90	1.22	0.53	0.20	3.00	0.33	0.65	−0.23
Er	6.94	4.06	0.63	0.17	12.4	1.87	0.73	−0.07
Fe	2.02	1.35	0.53	0.20	3.06	0.50	0.63	−0.18
Ge	1.06	−0.67	0.53	−0.01	1.28	0.46	0.57	−0.02
Mg	3.23	2.11	0.54	0.18	4.13	1.39	0.59	−0.04
Mo	2.52	1.61	0.51	0.18	3.48	0.81	0.58	−0.09
Nb	1.69	1.13	0.52	0.20	2.49	0.38	0.62	−0.23
Ni	3.41	2.10	0.54	0.17	5.00	1.23	0.60	−0.06
Pd	3.81	2.44	0.51	0.15	5.45	1.88	0.55	−0.02
Pt	2.95	1.61	0.47	0.12	4.58	0.69	0.51	−0.05
Te	12.3	6.72	0.54	0.11	17.6	7.38	0.55	0.05
ZnTe	1.87	1.24	0.52	0.20	2.66	0.54	0.62	−0.20
ZnSe	1.12	0.65	0.50	0.17	1.33	0.67	0.52	0.04
ZnS	1.02	0.55	0.48	0.14	1.20	0.56	0.49	0.02
SiO2	0.94	0.42	0.52	0.14	0.91	0.38	0.53	−0.02
Si	1.79	1.26	0.50	0.21	2.27	0.81	0.57	−0.14

experimental data. Because the previous definitions of SEP were different, there are large deviations among earlier calculated results. We conclude that the net excitation probability for the electron inside the solid including the inhibition of the bulk excitations and the induced surface excitations is nonvanishing for almost all materials. The most effective empirical formula is chosen from among four formulas in common use. This formula was fitted to the calculated SEPs for different energies and angles, and the best-fit material-dependent parameters were obtained. Our SEP database can be directly used in various problems of surface excitation, especially for determining IMFP parameters with EPES methods.

Acknowledgements

This work was supported by the National Natural Science Foundation of China (Grant Nos. 11074232 and 11274288), '973' projects (Nos. 2011CB932801 and 2012CB933702) and '111' project. We thank Supercomputing Center of USTC for support to parallel computations.

References

[1] A. Dubus, A. Jablonski, S. Tougaard, *Prog. Surf. Sci.* **2000**, *63*, 135.
[2] W. de la Cruz, F. Yubero, *Surf. Interface Anal.* **2007**, *39*, 460.
[3] G. Gergely, *Prog. Surf. Sci.* **2002**, *71*, 31.
[4] K. Olejnik, J. Zemek, W. S. M. Werner, *Surf. Sci.* **2005**, *595*, 212.
[5] F. Yubero, S. Tougaard, *Phys. Rev. B* **1992**, *46*, 2486.
[6] A. C. Simonsen, F. Yubero, S. Tougaard, *Phys. Rev. B* **1997**, *56*, 1612.
[7] S. Tanuma, S. Ichimura, K. Goto, *Surf. Interface Anal.* **2000**, *30*, 212.
[8] J. Zemek, P. Jiricek, B. Lesiak and A. Jablonski, *Surf. Sci.* **2004**, *562*, 92.
[9] C. J. Tung, Y. F. Chen, C. M. Kwei, T. L. Chou, *Phys. Rev. B* **1994**, *49*, 16684.
[10] Y. F. Chen, C. M. Kwei, *Surf. Sci.* **1996**, *364*, 131.
[11] K. Salma, Z. J. Ding, H. M. Li, Z. M. Zhang, *Surf. Sci.* **2006**, *600*, 1526.
[12] C. M. Kwei, S. J. Hwang, Y. C. Li, C. J. Tung, *J. Appl. Phys.* **2003**, *93*, 9130.
[13] Y. C. Li, Y. H. Tu, C. M. Kwei, C. J. Tung, *Surf. Sci.* **2005**, *589*, 67.
[14] R. H. Ritchie, *Phys. Rev.* **1957**, *106*, 874.
[15] R. F. Egerton, *Electron Energy-Loss Spectroscopy in the Electron Microscope*, 2nd edition, Plenum, New York, **1996**.
[16] N. Pauly, S. Tougaard, *Surf. Sci.* **2007**, *601*, 5611.
[17] Z. J. Ding, *J. Phys. Condens. Matter* **1998**, *10*, 1733.
[18] Z. J. Ding, *J. Phys. Condens. Matter* **1998**, *10*, 1753.
[19] Z. J. Ding, *Phys. Rev. B* **1997**, *55*, 9999.
[20] B. Da, S. F. Mao, Z. J. Ding, *J. Phys. Condens. Matter* **2011**, *23*, 395003.
[21] Y. C. Li, Y. H. Tu, C. M. Kwei, C. J. Tung, *Surf. Sci.* **2005**, *589*, 67.
[22] F. Flores, F. Garcia-Moliner, *J. Phys. C* **1979**, *12*, 907.
[23] H. Kanazawa, *Prog. Theor. Phys.* **1961**, *26*, 851.
[24] N. Takimoto, *Phys. Rev.* **1965**, *146*, 36674.
[25] J. Harris, R. Jones, *J. Phys. C* **1973**, *6*, 3585.
[26] J. Harris, R. Jones, *J. Phys. C* **1974**, *7*, 3751.
[27] C. M. Kwei, S. J. Hwang, Y. C. Li, C. J. Tung, *J. Appl. Phys.* **2003**, *93*, 9130.
[28] R. H. Ritchie, A. Howie, *Phil. Mag. A* **1977**, *36*, 463.
[29] E. D. Palik (Ed.), *Handbook of Optical Constants of Solids*, Academic, Orlando, FL, **1985**.
[30] C. M. Kwei, Y. F. Chen, C. J. Tung, J. P. Wang, *Surf. Sci.* **1993**, *293*, 202.
[31] N. Pauly, S. Tougaard, *Surf. Sci.* **2008**, *602*, 1974.
[32] C. M. Kwei, Y.C. Li, C. J. Tung, *Surf. Sci.* **2006**, *600*, 3690.
[33] W. S. M. Werner, W. Smekal, C. Tomastik, H. Stori, *Surf. Sci.* **2001**, *486*, L461.
[34] Y. F. Chen, *Surf. Sci.* **2002**, *519*, 115.
[35] G. Gergely, M. Menyhard, S. Gurban, J. Toth, D. Varga, *Surf. Interf. Anal.* **2004**, *36*, 1098.
[36] W. S. M. Werner, *Surf. Interf. Anal.* **2003**, *35*, 347.
[37] W. S. M. Werner, L. Kover, S. Egri, J. Toth, D. Varga, *Surf. Sci.* **2005**, *585*, 85.
[38] A. Jablonski, J. Zemek, *Surf. Sci.* **2007**, *601*, 3409.
[39] G. Gergely, S. Gurban, M. Menyhard, A. Jablonski, J. Zemek, K. Goto, *Surf. Interf. Anal.* **2011**, *4*, 1365.
[40] T. Nagatomi, S. Tanuma, K. Goto, *Surf. Interf. Anal.* **2010**, *42*, 1537.
[41] N. Pauly, S. Tougaard, *Surf. Interf. Anal.* **2008**, *40*, 731.
[42] N. Pauly, S. Tougaard, *Surf. Interf. Anal.* **2009**, *41*, 735.